# 13A.5 THE EXTRATROPICAL TRANSITION OF HURRICANE HELENE (2006): OBSERVATION OF STRUCTURAL EVOLUTION AND OPERATIONAL MODEL EVALUATION USING QUIKSCAT

Michael J. Brennan*, Jamie R. Rhome, and Richard D. Knabb
NOAA/NWS/NCEP National Hurricane Center (NHC), Miami, FL

## 1. INTRODUCTION

The evolution of the horizontal wind field of a tropical cyclone (TC) as it undergoes extratropical transition (ET) determines the distribution of hazardous conditions around the cyclone as it moves to higher latitudes. While the scarcity of *in situ* observations over the open oceans makes analysis of this evolution difficult to observe, ocean surface vector wind (OSVW) data from the NASA QuikSCAT scatterometer can provide spatially consistent snapshots of the cyclone's wind field during the ET process. QuikSCAT retrievals are usually more reliable in the periphery of TCs, outside areas of heavy precipitation (e.g., Brennan and Knabb 2007). However, as convection diminishes near the center of the TC during ET, rain contamination effects decrease and QuikSCAT retrievals near the cyclone core become more useful for estimating cyclone intensity (maximum sustained surface wind). In this study the evolution of the wind field structure during the ET of Atlantic basin Hurricane Helene (2006) is examined using QuikSCAT.

According to the final NHC best track analysis, Helene reached a peak intensity of 105 kt on 18 September and weakened to 70 kt as the storm turned toward the northeast on 22 September (Brown 2006). During the early stages of ET (22–24 September), Florida State University (FSU) cyclone phase space diagrams (Hart 2003) indicate that Helene maintained a deep warm core while the circulation became more asymmetric. Early on 23 September, Helene attained a secondary peak in intensity of 80 kt, as indicated by QuikSCAT data in a convection-free area to the southwest of the center. As Helene intensified, the azimuthally averaged radius of 34-kt winds around the cyclone increased by ~40%. The wind radii continued to expand as Helene gradually weakened to 65 kt early on 24 September.

Several QuikSCAT passes over Helene during ET are examined, and the evolution of the 34-kt wind field of the cyclone is documented. Additionally, operational numerical weather prediction (NWP) model forecasts of the outer wind field of Helene during this period are evaluated. In particular, this study examines the sensitivity of model surface wind field forecasts of Helene during ET to (i) differences in the initial vortex structure between three global models and (ii) the varying degree of interaction of Helene with a mid-latitude upper-level trough in forecasts from these models

Implications of these results for operational forecasting of wind radii during ET are discussed, along with the potential utility of future OSVW missions for observing these wind field evolutions.

*Current affiliation: NOAA/NWS/NCEP Hydrometeorological Prediction Center
*Corresponding author address:*
Dr. Michael J. Brennan
5200 Auth Rd., Camp Springs, MD 20746
Email: Michael.J.Brennan@noaa.gov

## 2. QUIKSCAT DESCRIPTION

The SeaWinds scatterometer onboard QuikSCAT is a Ku-band scatterometer that estimates OSVW by measuring the return of backscatter due to centimeter-scale capillary waves on the ocean surface. QuikSCAT nominally provides wind retrievals with a horizontal resolution of 25 km, and since 2003 near-real time (NRT) 12.5-km retrievals have been available. The NRT QuikSCAT retrievals available at the National Hurricane Center (NHC) are processed at the National Oceanic and Atmospheric Administration/National Environmental Satellite, Data, and Information Service (NOAA/NESDIS) using the NRT retrieval process described by Hoffman and Leidner (2005). These data are displayed on the NOAA/National Centers for Environmental Prediction (NCEP) Advanced Weather Interactive Processing System (N-AWIPS) workstations used by NHC forecasters.

One of the primary limitations of QuikSCAT wind data is contamination due to the effects of rain, particularly in TCs where the strongest winds are most often found in regions of deep convection and high rainfall rates. However, in many hurricanes, the radius of 34-kt winds often extends beyond the region of heavy rainfall near the TC core. As a result, QuikSCAT is a critical tool for analyzing the structure of the outer wind field of a TC, frequently providing the only information on outer wind radii to NHC forecasters for TCs outside the range of aircraft reconnaissance (Brennan and Knabb 2007). Accurate analyses and forecasts of the outer wind field of a TC are important to marine interests and the timing and placement of tropical cyclone watches and warnings for coastal areas.

## 3. OBSERVATIONAL ANALYSIS

According to the threshold value of Evans and Hart (2003), ET begins when cyclone phase space parameter B, which measures the lower-tropospheric thickness (thermal) asymmetry across the cyclone, exceeds 10 m. Analyzed phase space diagrams from the GFS, UKMET, and NOGAPS (Fig. 1) indicate that B first exceeded the 10 m threshold between 0000 UTC and 1200 UTC 22 September. During the early stages of ET (22–23 September), Helene experienced moderate weakening as shown in the NHC best track (Fig. 2). Conventional geostationary satellite imagery indicates that Helene began ET on 22 September, as the cyclone developed an increasingly asymmetric convective pattern and frontal-like structure (Fig. 3). Dry, stable air wrapping around the southwestern periphery of the cyclone early on 22 September began to erode the inner-core deep convection. The appearance of cold-air stratocumulus clouds southwest of the cyclone suggest the presence of cold advection while the displacement of deep convection poleward of an apparent warm frontal band northeast of Helene indicates strong warm advection in the eastern semicircle of the cyclone. A weaker cold frontal cloud band trailing equatorward of Helene is also evident in geostationary satellite imagery (Fig. 3). Moreover, upper-level cirrus outflow associated with deep convection along the warm frontal band began displaying an increasingly sharp northern edge as it converged with the polar jet. The aforementioned structural changes, as implied by satellite imagery, closely match the early stages of ET in the conceptual model outlined in Klein et. al (2000).

Early on 23 September, Helene attained a secondary peak in intensity of 80 kt as determined by a QuikSCAT pass near 0916 UTC 23 September (Fig. 4). The strongest winds were located within a convection-free area over the southwestern semicircle as indicated by satellite imagery. Additionally, the QuikSCAT pass showed developing frontal structure indicated by the area of relatively weaker winds over the northeastern quadrant coupled with a “crescent” shaped area of hurricane force winds over the southwestern quadrant (Fig. 11d). This pattern closely matches that found in a QuikSCAT-based composite study of hurricane force extratropical cyclones (Von Ahn et al. 2006, their Fig. 11), and is highly suggestive of a cyclone undergoing ET. The presence of deep convection over the low-level circulation, albeit limited, along with the appearance of frontal structure during the second peak in intensity indicates the presence of both diabatic and baroclinic forcing during this period of re-strengthening. By 1200 UTC 24 September, Helene had lost most of its inner-core convection and more definitive frontal structure was apparent in cloud patterns from geostationary satellite imagery. Moreover, a QuikSCAT pass near 0900 UTC 24 September showed that the strongest winds had become well removed from the center (Fig. 5). Accordingly, the NHC best track indicates that Helene became extratropical at 1800 UTC 24 September (Brown 2006).

Still, microwave data (not shown) and model analyses from the GFS, UKMET, and NOGAPS continued to show a warm-core, albeit less deep, structure on 24 and 25 September (Fig. 6). Based on this information, it appears that Helene may have become instantly warm secluded, largely bypassing a cold-core phase during ET.

## 4. OPERATIONAL MODEL EVALUATION

Forecasts of the structure of the 34-kt wind field from the global models run by the U.S. National Weather Service (GFS), U.S. Navy (NOGAPS), and the U.K. Met Office (UKMET) initialized at 0000 UTC 22 September, the approximate time at which ET began, are evaluated here using data from QuikSCAT passes through 0000 UTC 24 September. These model data were examined on 1° global grids identical to those operationally available to NHC forecasters. This model cycle was chosen since it encompassed most of the ET process and several QuikSCAT passes were available for evaluation from 22–24 September.

At the initial analysis time of 0000 UTC 22 September, the NHC best track indicates Helene had maximum sustained winds of 75 kt and a central pressure of 970 hPa (Brown 2006). Between the three models, the analyzed structure of Helene varies widely (Fig. 7). The GFS analysis shows the deepest cyclone, with a central pressure of 983 hPa, and a large area of 34 kt wind encircling the center (Fig. 7a). The NOGAPS and UKMET initial analyses of the cyclone are much weaker, with central pressures of 997 hPa and 993 hPa, respectively, and a much weaker wind field around the cyclone (Fig. 7b,c). In particular, the UKMET analysis is quite weak, showing 34-kt winds only in the eastern semicircle (Fig. 7c). Compared to the QuikSCAT pass at 2227 UTC 21 September (Fig. 7d) [1], the wind field from the GFS most closely resembles the QuikSCAT observations, showing a continuous area of 34-kt winds encircling the cyclone and a smaller area of 50-kt winds, largely in the eastern semicircle.

As an approximation of the overall size of the outer wind field, azimuthally averaged 34-kt wind radii[2] from each model are compared to averages computed from QuikSCAT data closest to the valid forecast times and the final NHC best track wind radii analysis in Figure 8. At the initial time, only the GFS model (184 nm) is close to the NHC analysis (190 nm) or QuikSCAT (213 nm), with the NOGAPS (119 nm) and UKMET (53 nm) showing a much smaller wind field around Helene at this time.

At 1200 UTC 22 September, 12-h forecasts from the NOGAPS and UKMET continue to be underdone in their depiction of the outer wind field of Helene, while the GFS compares more favorably to the QuikSCAT

[1] QuikSCAT data are assimilated into all three models examined here.
[2] The azimuthal average was computed by averaging the maximum radius of 34-kt winds in each quadrant of the cyclone.

pass from 0941 UTC 22 September (Fig. 9). During the period from 0000 to 1200 UTC, the QuikSCAT data and NHC best track analysis show little change or a slight increase in the azimuthally averaged 34-kt wind radii (Fig. 8). The GFS matches the slight increase seen, and is very close to QuikSCAT and the NHC best track analysis at this time. While the NOGAPS and UKMET continue to lag observations considerably, both models show an increase in the size of the outer wind field compared to the 0000 UTC 22 September analysis.

By 0000 UTC 23 September, the 24-h forecasts from the global models continue to show the GFS with the largest outer wind field, comparing more favorably to the QuikSCAT analysis from a pass at 2159 UTC 22 September (Fig. 10a,d). The NOGAPS (Fig. 8b) shows a large increase in the extent of 34-kt wind radii from the 12-h forecast; the azimuthally-averaged 34-kt wind radii increase to 208 nm from 139 nm only 12 h earlier while the model forecasts the cyclone to deepen. The UKMET continues to lag behind in its forecast of the outer wind structure, showing 34-kt winds mostly south and east of the cyclone center (Fig. 10c), despite forecasting a cyclone 1 hPa deeper than the NOGAPS.

At the 36-h forecast time, valid at 1200 UTC 23 September, the depiction of the outer wind field in the GFS model (Fig. 11a) is remarkably accurate when compared to the QuikSCAT pass at 0916 UTC 23 September (Fig. 11d), showing an expansion of the 34-kt winds in the western semicircle, and the smallest extent of winds northeast of the center. The NOGAPS and UKMET (Fig. 11b,c) both hint at the development of this asymmetry, but under-forecast the extent of the 34-kt winds compared to QuikSCAT. Additionally, at this time the reduction of convection near the core of Helene increased confidence in the 80-kt wind maximum indicated by QuikSCAT south of the center at this time. It is noteworthy that the formation of hurricane-force winds in the southwest quadrant of the cyclone at this time was forecasted by the GFS model (Fig. 11a).

Finally, at 0000 UTC 24 September, the 48-h forecasts from the models continue to depict the asymmetric structure of the 34-kt wind field around Helene, but the UKMET continues to under-represent the outer wind field more than the GFS or NOGAPS (Fig. 12). Some of the large differences in the outer wind field structure by this time between the models is likely related to the deeper cyclone depicted by the GFS at this time (central pressure of 969 hPa) compared to the UKMET (981 hPa) and NOGAPS (983 hPa); the NHC best track analysis indicates Helene had a central pressure of 964 hPa at this time (Brown 2006). Interestingly, the trend of a larger outer wind field, despite a weaker cyclone, continues to be seen in the NOGAPS relative to the UKMET. At this time, the azimuthally averaged 34-kt wind radii from the GFS continues to be most accurate compared to both the QuikSCAT and NHC best track analysis, while the NOGAPS and UKMET forecast wind fields are 15% and 27% smaller, respectively.

Over the 48-h period, the NHC best track analysis showed an increase in the azimuthally averaged 34-kt wind radii of almost 52% over the analysis at 0000 UTC 22 September. QuikSCAT shows an increase of about 39% through the same period. This difference in the increase between QuikSCAT data and the NHC analysis is likely due to some of the outermost 34-kt winds in the QuikSCAT at earlier times being judged as rain inflated. The GFS, NOGAPS, and UKMET model forecasts showed an increase of the azimuthally averaged 34-kt wind radii of 41%, 85%, and 256%, respectively. The GFS increase is similar to that shown by QuikSCAT, while even the very large increases in the NOGAPS and UKMET were unable to properly represent the final wind field structure and its large size, likely due to shortcomings in the initial analysis. The weaker initial cyclone in the NOGAPS and UKMET is somewhat surprising, given that both of these models use a bogussing technique, while the GFS does not. Overall, the GFS model produced a remarkably accurate forecast of both central pressure and wind field structure as Helene was undergoing ET for the model cycle evaluated here.

The degree of interaction of Helene with the mid-latitude flow was evaluated, and results from forecast hour 48 (0000 UTC 24 September) are presented here (Fig. 13). At this time, all three models forecast a configuration of the 200-hPa flow that is similar to that analyzed by the GFS at the valid time (Fig. 13d). The largest differences between the model forecasts appear to be related to the structure of the tropical cyclone itself, with the GFS showing the strongest vortex, and the NOGAPS the weakest. However, the jet maximum north of Helene is weaker in the NOGAPS, and in this model the cyclone is farther removed from the equatorward jet entrance region than either the UKMET or the GFS forecast. This examination suggests that in this case, the structural differences seen between the models examined here during the ET of Helene were largely due to differences in initial cyclone structure in the model analyses than large differences in the degree of interaction of the TC with the baroclinic flow.

A vertical cross section though the cyclone showing potential vorticity (PV) is taken at the analysis and 48-h forecast times from the GFS and UKMET to examine differences in the vertical structure of the vortex and its interaction with the tropopause [3]. Potential vorticity is the product of the absolute vorticity and the static stability (Rossby 1940; Ertel 1942). In the Northern Hemisphere high- (low-) PV

[3] This comparison was not performed for the NOGAPS, since the operationally received NOGAPS model grids at NHC do not include all the necessary fields.

air is associated with cyclonic (anticyclonic) absolute vorticity and/or high (low) values of static stability (Hoskins et al.1985).

At the analysis time (0000 UTC 22 Sep.), the differences in the structure of Helene's vortex between the GFS and UKMET are striking. The GFS (Fig. 14a) depicts a deeper, stronger, and larger vortex than the UKMET (Fig. 14b), with maximum PV values exceeding 4 potential vorticity units (PVU)[4] in the lower-troposphere in the GFS, compared to 3 PVU in the UKMET. Additionally, in the GFS analysis, Helene is already interacting with the stratospheric PV reservoir. In contrast, the shallower vortex in the UKMET analysis shows no interaction with the tropopause PV gradient. These large differences in the analyzed Helene vortex continue to suggest that these structural differences in the model analyses played a major role in the variations seen in the differing structural evolution in the models during ET.

Large structural differences persist at the 48-h forecast time. The GFS (Fig. 15a) shows a strong but decidedly more asymmetric PV tower associated with Helene and a lowering of the dynamic tropopause below the 300-hPa level upstream of the cyclone. The UKMET forecast (Fig. 15b) continues to show a shallower and weaker PV tower, albeit one that is showing signs of interacting with the tropopause PV gradient, evident in the lowering (raising) of the 1.5 PVU surface upstream (downstream) of Helene.

**5. SUMMARY**

Overall, the three global models examined here, GFS, UKMET, and NOGAPS show a large variation in the forecast structure of Hurricane Helene as it progressed through ET. The variations in the forecast of cyclone structure appear to be largely due to differences in the initial analysis of the cyclone vortex, with the GFS showing a much more robust vortex in the analysis than the UKMET or NOGAPS. The lack of initial and forecast structure in the wind field of Helene in the NOGAPS and UKMET is somewhat surprising, since both models utilize a synthetic "bogus" vortex in their analysis scheme. Despite this fact, their analyzed cyclone was substantially weaker and smaller than that in the GFS at 0000 UTC 22 September. The reasons for the weaker initial vortex in the UKMET and NOGAPS are unknown, but should be the focus of future study, as these analysis differences can have a significant impact on the evolution of the TC wind field structure and intensity during ET, and can be particularly difficult to diagnose in the time-constrained operational forecast environment.

Forecasts of 34-kt wind field structure from the GFS were quite accurate both qualitatively and in the quantitative increase in the wind radii during the period examined when compared to QuikSCAT and the NHC best track analysis. Both the NOGAPS and UKMET under-forecasted the extent of the 34-kt winds around Helene compared to both observations and the GFS forecast during the period examined here. The NOGAPS model showed a large increase in the 34-kt wind field by forecast hour 24, while the UKMET model delayed its largest increase until forecast hour 36.

The relative location of the cyclone vortex to the upper-level mid-latitude flow is similar, with all three models showing Helene in the equatorward-entrance region of the 200-hPa jet by forecast hour 48. This suggests that differences in the large scale flow at higher latitudes were not the main factors in differences between the structural evolution of Helene in this forecast cycle. It seems more likely that the degree of interaction with the baroclinic flow in this case was determined by the initial and forecast structure of the TC itself. For example, the weaker, shallower TC vortex in the UKMET does not undergo the same degree of interaction with the tropopause PV gradient as seen in the GFS. These differences in the size and intensity of the TC vortex also play a role in determining the post-transition intensity and structure of the cyclone (Hart et al. 2006), so variation in the initial analysis of the cyclone can heavily impact the track, intensity, and structure of a transitioning cyclone in the model forecast.

The increased focus on ET in recent years has highlighted the tremendous need for an improvement in the coverage and quality of wind observations within the environment of cyclones undergoing ET. The finding here that major model differences in the structure of Helene during ET were largely related to differences in the initial analysis of the cyclone vortex further underscores the need to increase the quantity and quality of data available in the core regions of TCs. These data are vital for input into data assimilation schemes to improve model analyses, verify increasingly higher-resolution model forecasts of TC evolution, and for subjective analysis, forecast, and warning applications.

As mentioned earlier, QuikSCAT often provides the only complete snapshot of the cyclone wind field in open-ocean TCs; and this instrument has already exceeded its life expectancy. The failure of QuikSCAT would leave only the European Space Agency's Advanced Scatterometer (ASCAT) to provide wind retrievals of similar quality in the TC environment. The coverage of ASCAT is only about 60% of QuikSCAT, and ASCAT retrievals will be performed with 50-km resolution, with post-processing techniques resulting in the availability of 25-km retrievals as well. Therefore, relying on ASCAT alone will result in a decrease in resolution and coverage relative to QuikSCAT in passes over TCs in the future.

[4] 1 PVU = $10^{-6}$ $m^3$ $s^{-1}$ K $kg^{-1}$

A multi-satellite platform, such as the extended ocean vector winds mission (XOVWM) recently recommended to NOAA by the National Academy of Sciences' *Decadal Survey* would provide a substantial increase in both the quality and quantity of remotely sensed ocean surface vector wind data for the real time observation of these and other extreme weather events.

## 6. ACKNOWLEDGEMENTS

Thanks to Mr. Greg McFadden of the Ocean Prediction Center for providing the original code to create GEMPAK grid files from QuikSCAT wind retrievals.

## 7. REFERENCES

Brennan, M. J., and R. D. Knabb, 2006: Operational evaluation of QuikSCAT ocean surface vector winds in tropical cyclones at the Tropical Prediction Center/National Hurricane Center. Preprints, *11th Symposium on Integrated Observing and Assimilation Systems for the Atmosphere, Oceans, and Land Surface,* San Antonio, TX, Amer. Meteor. Soc. Available online at: http://ams.confex.com/ams/pdfpapers/117225.pdf.

Brown, D. P., 2006: Tropical cyclone report, Hurricane Helene, 12–24 September 2006. Available online at: http://www.nhc.noaa.gov/pdf/TCR-AL082006_Helene.pdf.

Ertel, H., 1942: Ein Neuer hydrodynamischer Wirbelsatz. *Meteor. Zeits.,* **59,** 271−281.

Evans, J. L., J.M. Arnot, and F. Chiaromonte, 2006: Evaluation of operational model cyclone structure forecasts during extratropical transition. *Mon. Wea. Rev.,* **134,** 3054–3072.

Evans, J. L., and R. E. Hart, 2003: Objective indicators of the life cycle evolution of extratropical transition of Atlantic tropical cyclones. *Mon. Wea. Rev.,* **131,** 909–925.

Hart, R. E., 2003: A cyclone phase space derived from thermal wind and thermal asymmetry. *Mon. Wea. Rev.,* **131,** 583–616.

Hart, R. E., J. L. Evans, and C. Evans, 2006: Synoptic composites of the extratropical transition life cycle of North Atlantic tropical cyclones: Factors determining posttransition evolution. *Mon. Wea. Rev.,* **134,** 553–578.

Hoffman, R.N., and S.M. Leidner, 2005, An introduction to the near-real-time QuikSCAT data. *Wea. Forecasting,* **20,** 476–493.

Hoskins, B. J., M. E. McIntyre, and A. W. Robertson, 1985: On the use and significance of isentropic potential vorticity maps. *Quart. J. Roy. Meteor. Soc.,* **111,** 877−946.

Klein, P. M., P. A. Harr, and R. L. Elsberry, 2000: Extratropical transition of Western North Pacific tropical cyclones: An overview and conceptual model of the transformation stage. *Wea. Forecasting,* **15,** 373–395.

Rossby, C.-G., 1940: Planetary flow patterns in the atmosphere. *Quart. J. Roy. Meteor. Soc.,* **66,** Supl., 68−87.

Von Ahn, J. M., J. M. Sienkiewicz, and P. S. Chang, 2006: Operational impact of QuikSCAT winds at the NOAA Ocean Prediction Center. *Wea. Forecasting,* **21,** 523–539.

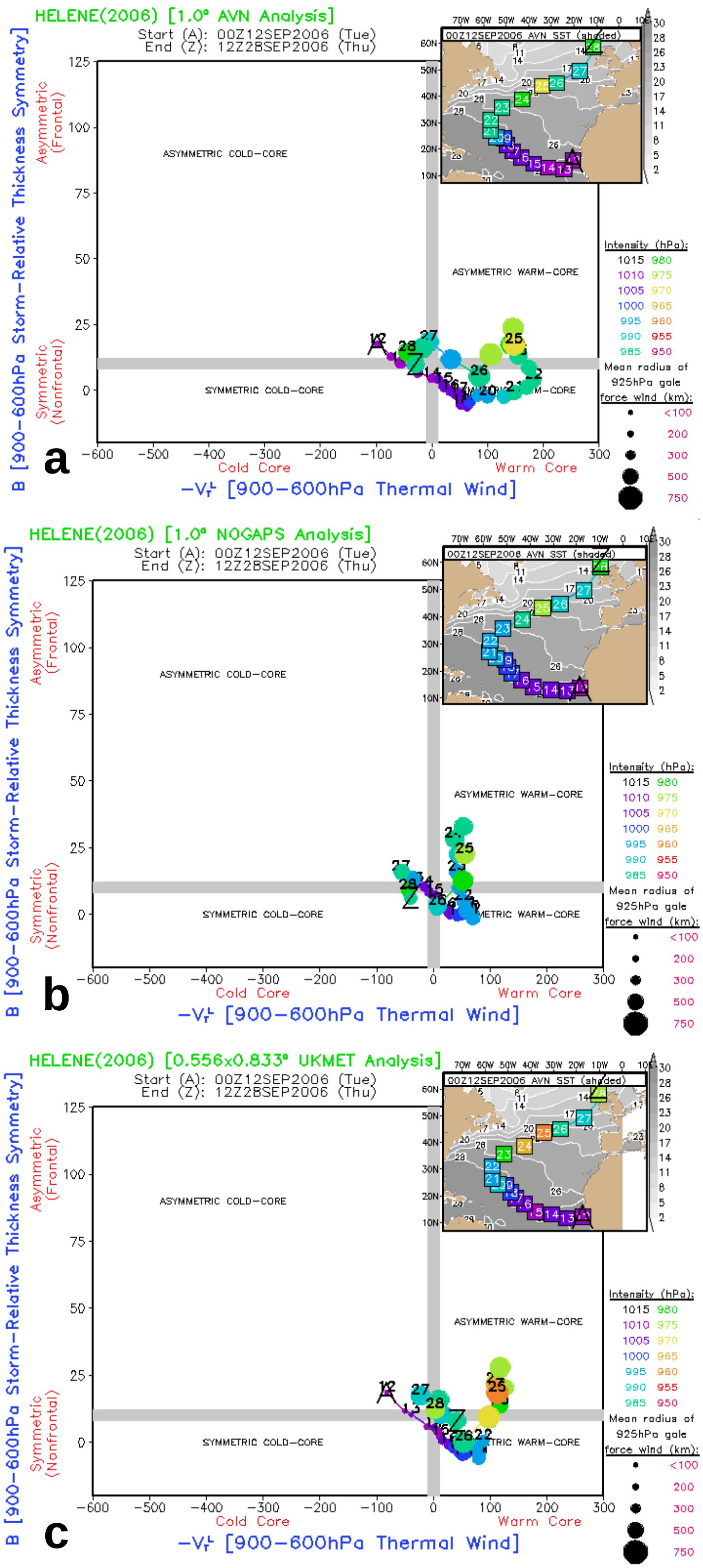


**Figure 1. Analyzed cyclone phase space diagrams from the (a) GFS, (b) NOGAPS, and (c) UKMET models for Helene showing frontal asymmetry (y-axis) and lower tropospheric circulation character (cold vs. warm core, x-axis). Images courtesy Bob Hart's cyclone phase space website.**

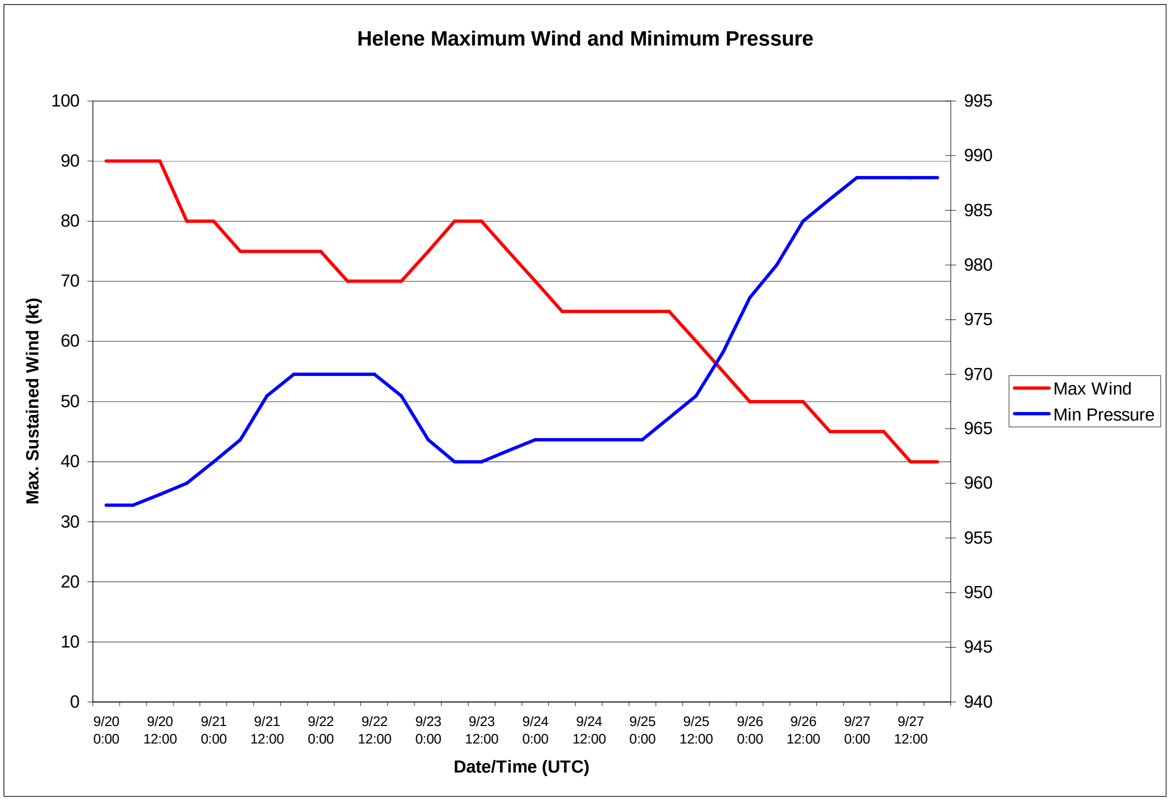


**Figure 2. NHC best track of maximum sustained wind (blue, kt) and minimum central pressure (red, hPa) of Helene (adapted from Brown 2006).**

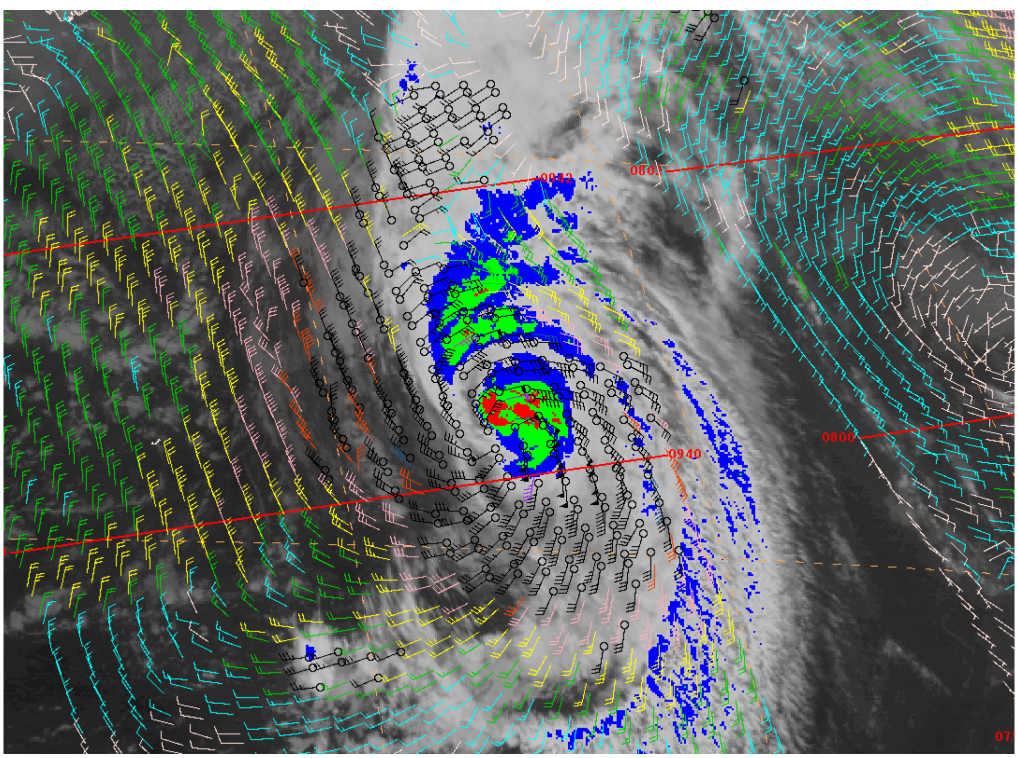

**Figure 3. 25-km QuikSCAT retrievals (barbs, kt) over Hurricane Helene from 0802 UTC 22 September and IR satellite imagery.**

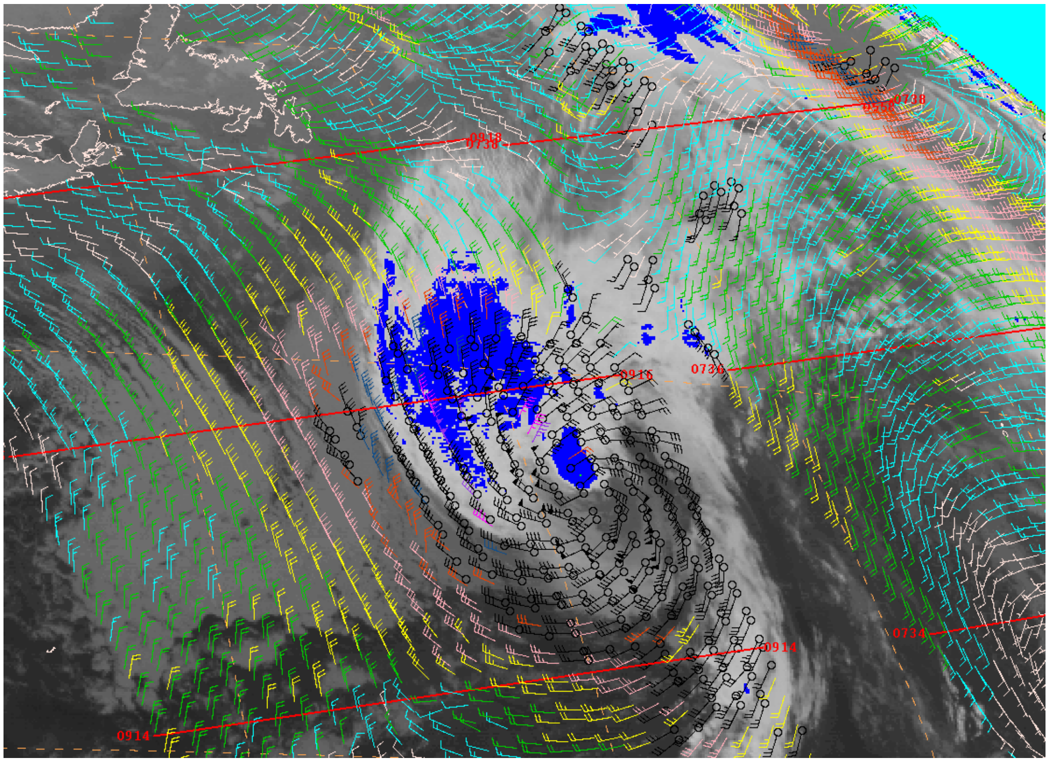

**Figure 4. As in Fig. 3, except from QuikSCAT pass at 0916 UTC 23 September.**

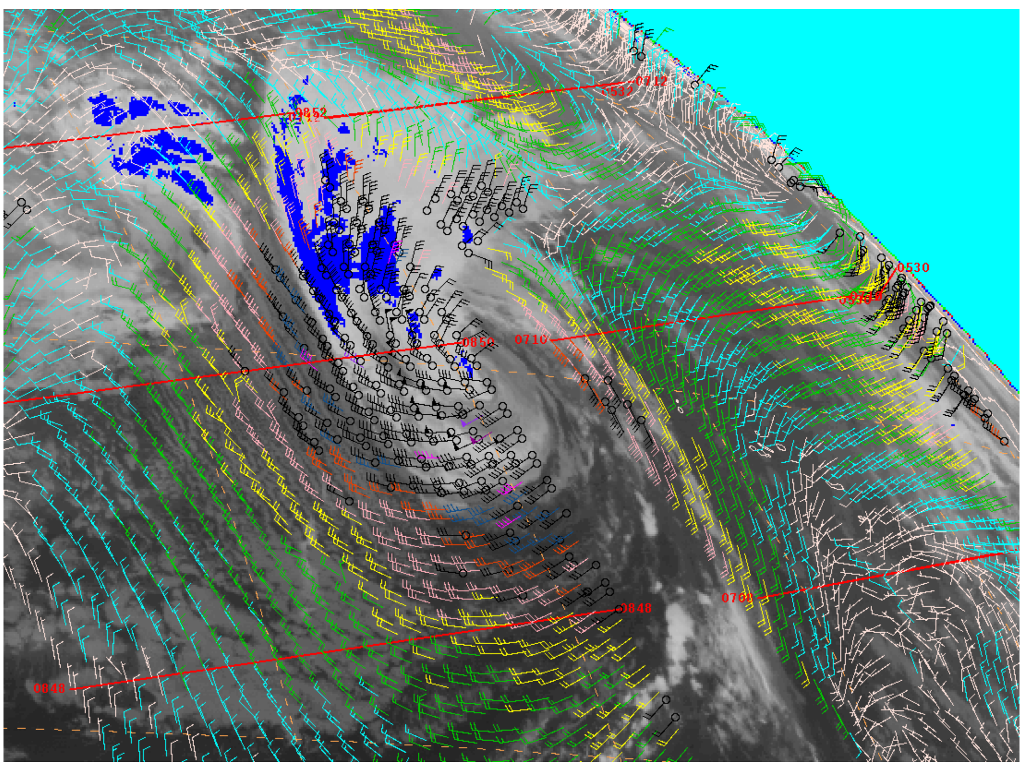

**Figure 5. As in Fig. 3, except from QuikSCAT pass from at 0851 UTC 24 September.**

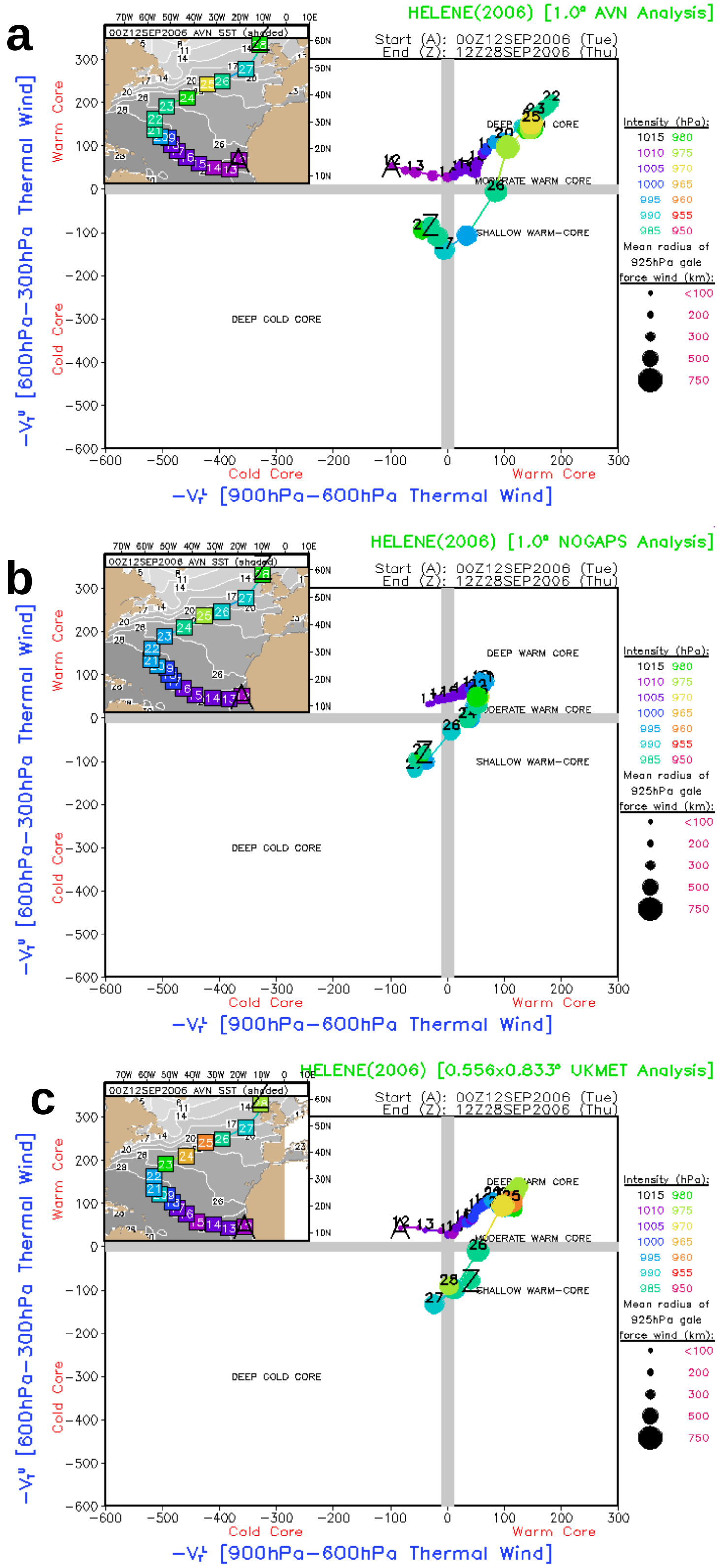


**Figure 6. As in Fig. 1, except showing mid- to upper-tropopsheric circulation character (cold vs. warm core) on y-axis.**

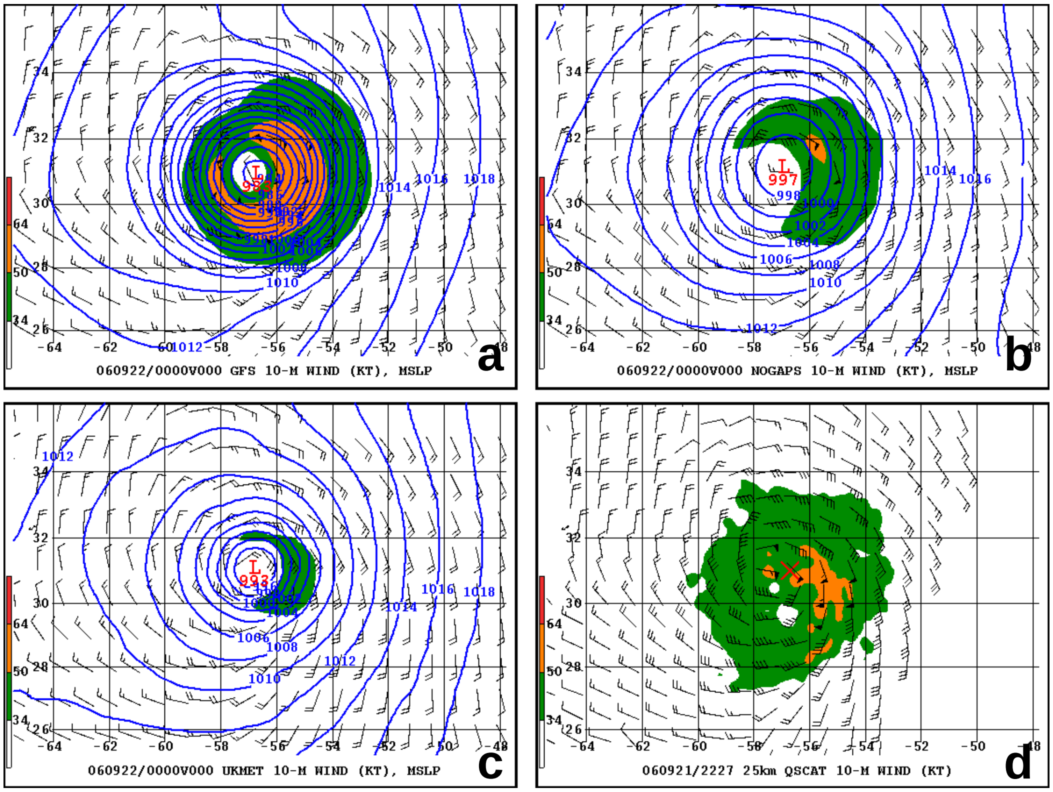


**Figure 7. Analysis of 10-m wind (barbs, kt), and isotachs (shaded, kt) valid at 0000 UTC 22 September 2006 from the (a) GFS, (b) NOGAPS, (c) UKMET models, and (d) QuikSCAT pass at 2227 UTC 21 September 2006. Wind speeds of 34 kt or greater are shaded according to the color scale.**

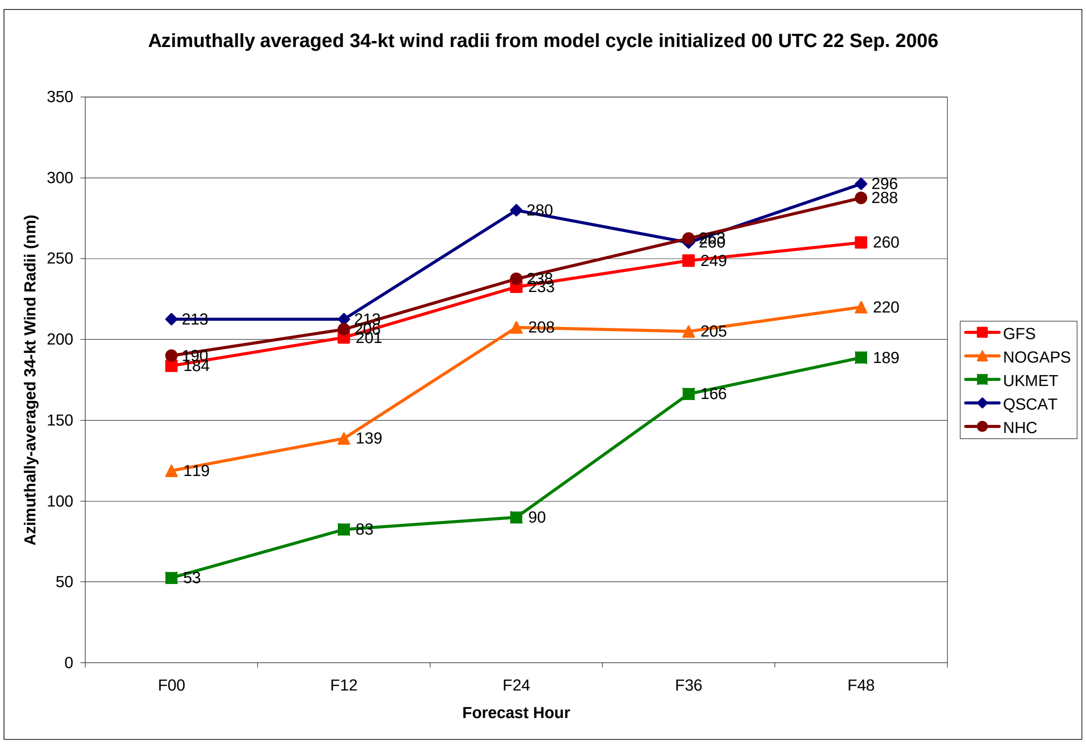


**Figure 8. Trend in azimuthally-averaged 34-kt wind radii (nm) from the GFS (red), NOGAPS (orange), and UKMET (green) models initialized at 0000 UTC 22 September 2006. Also shown are analyses at the verifying times from the final NHC best track (brown) and the closest QuikSCAT pass to the verifying times (blue).**

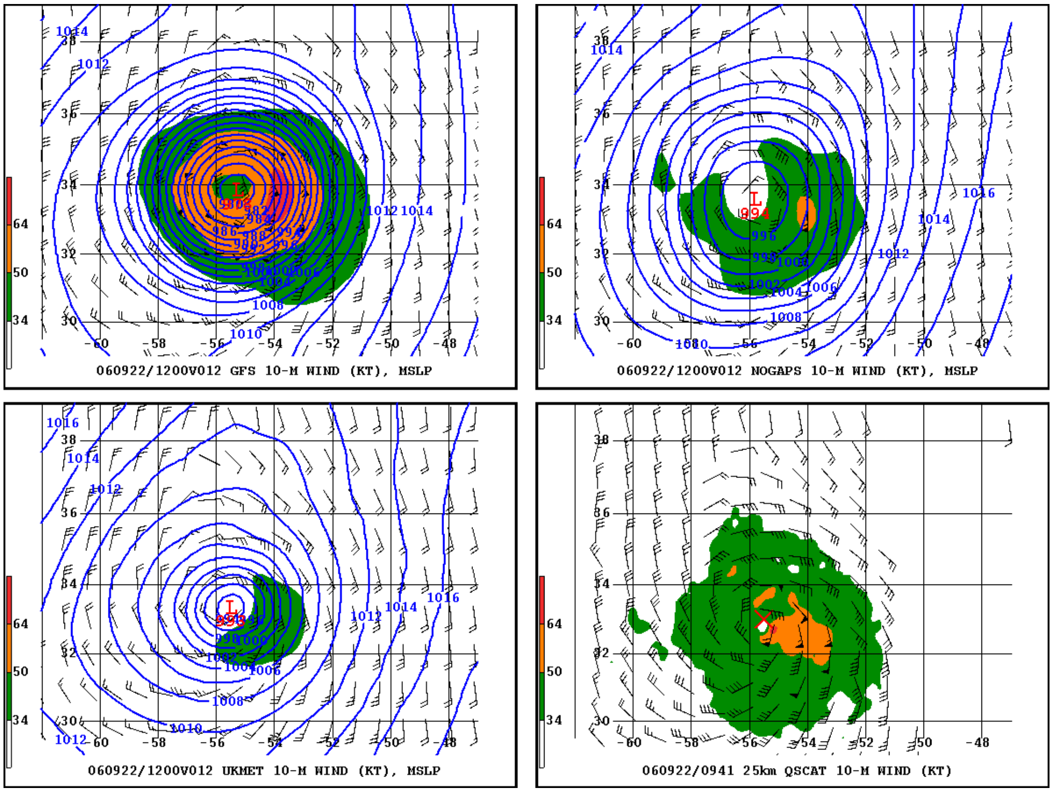


**Figure 9. As in Fig. 7, except 12-h forecast valid at 1200 UTC 22 September and QuikSCAT pass from 0941 UTC 22 September.**

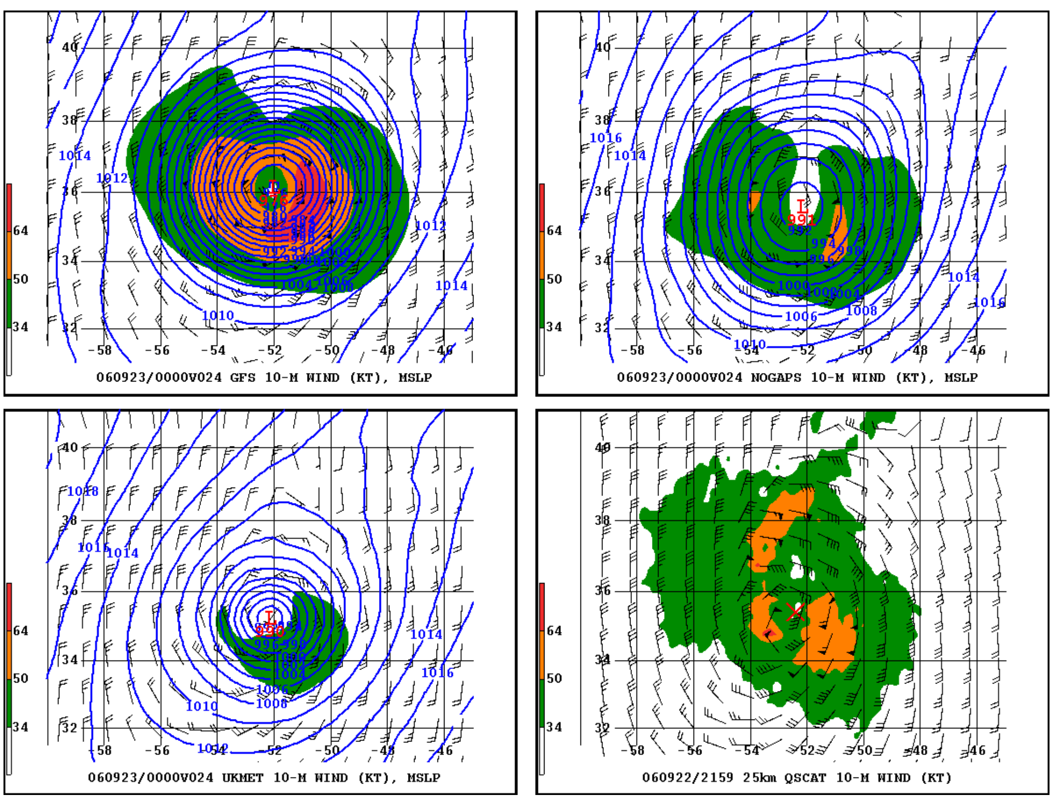


**Figure 10. As in Fig. 7, except 24-h forecast valid at 0000 UTC 23 September and QuikSCAT pass from 2159 UTC 22 September.**

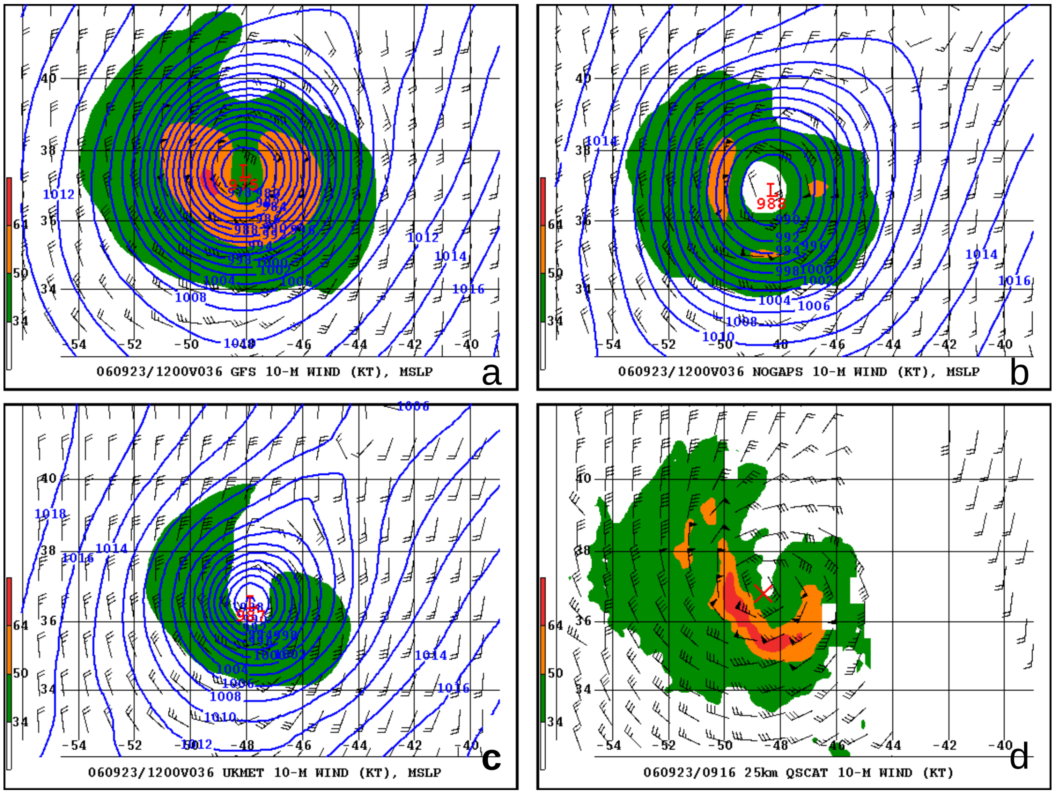


**Figure 11. As in Fig. 7, except 36-h forecast valid at 1200 UTC 23 September and QuikSCAT pass from 0916 UTC 23 September.**

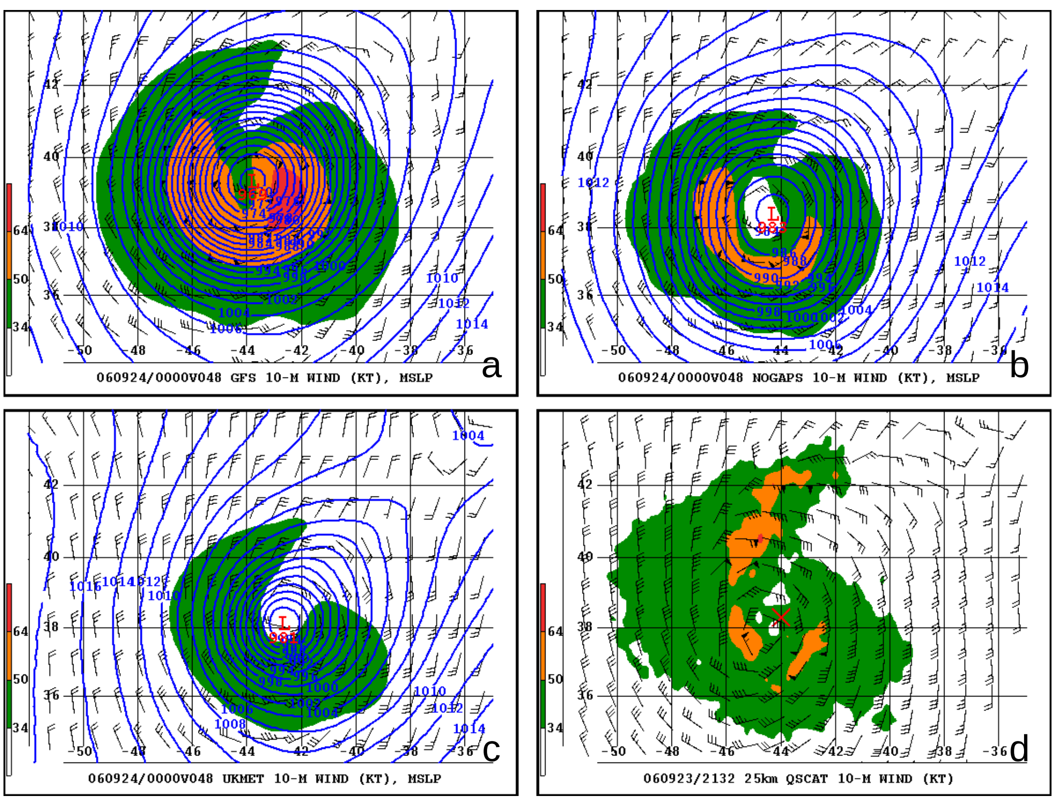


**Figure 12. As in Fig. 7, except 48-h forecast valid at 0000 UTC 24 September and QuikSCAT pass from 2132 UTC 23 September.**

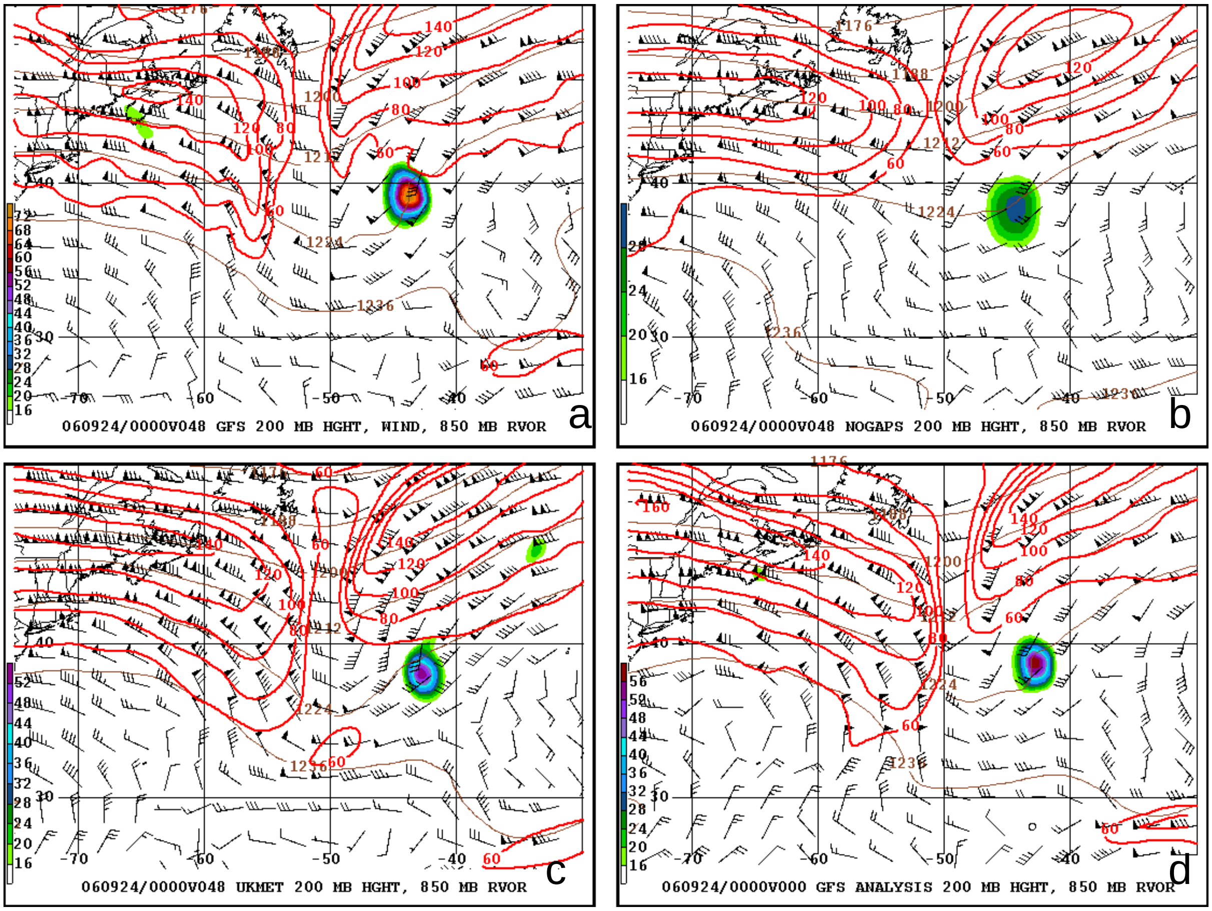


**Figure 13. 48-h forecast from (a) GFS, (b) NOGAPS, and (c) UKMET models and (d) GFS analysis valid at 0000 UTC 24 September of 850-hPa relative vorticity (shaded), 200-hPa height (brown contours every 12 dam), 200-hPa wind (barbs, kt), and isotachs (red contours, every 20 kt starting at 60 kt).**

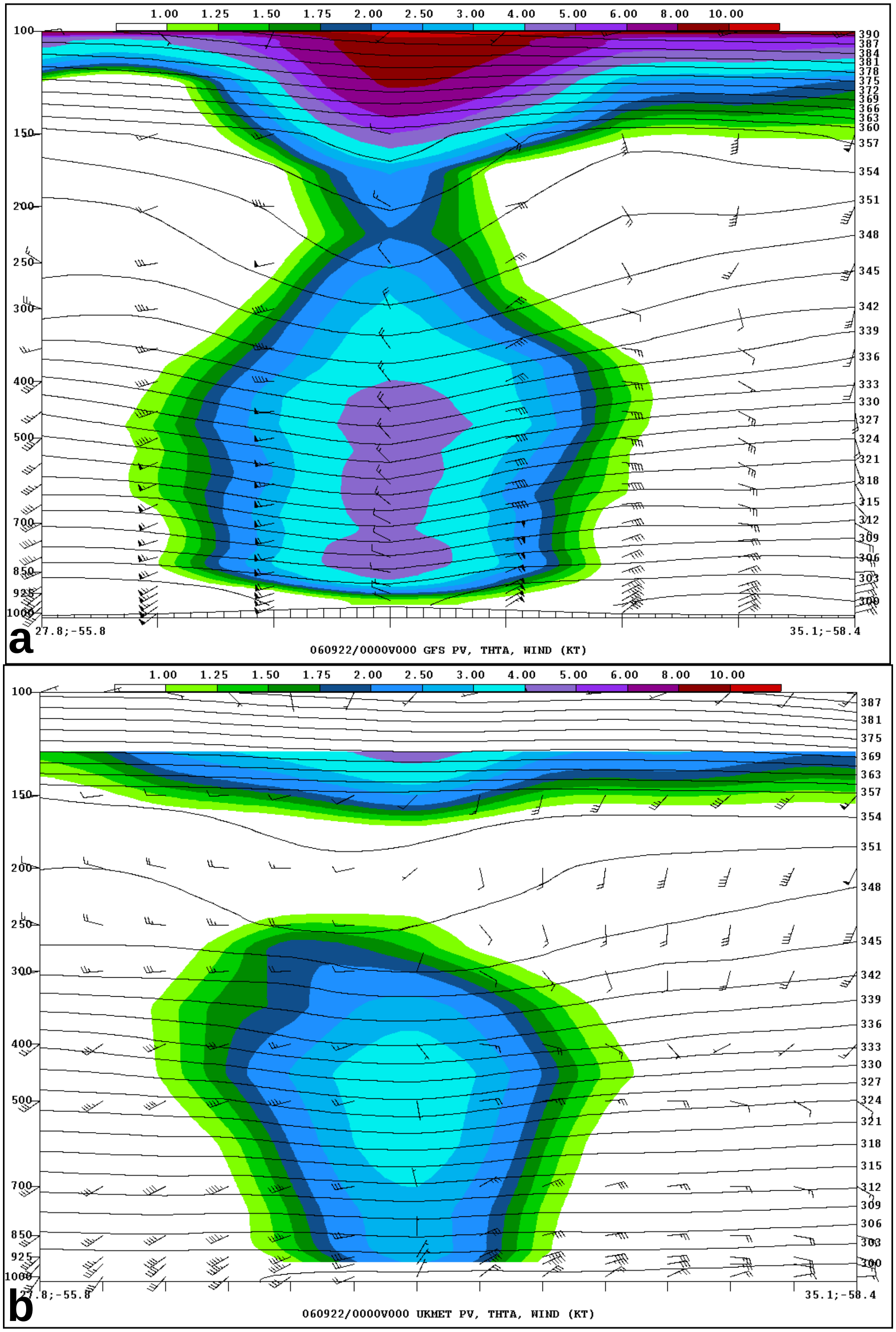


**Figure 14. Cross section from 27.8°N 55.8°W to 35.1°N 58.4°W depicting potential vorticity (shaded, PVU), potential temperature (solid contours) and wind (barbs, kt) from (a) GFS and (b) UKMET analysis valid at 0000 UTC 22 September.**

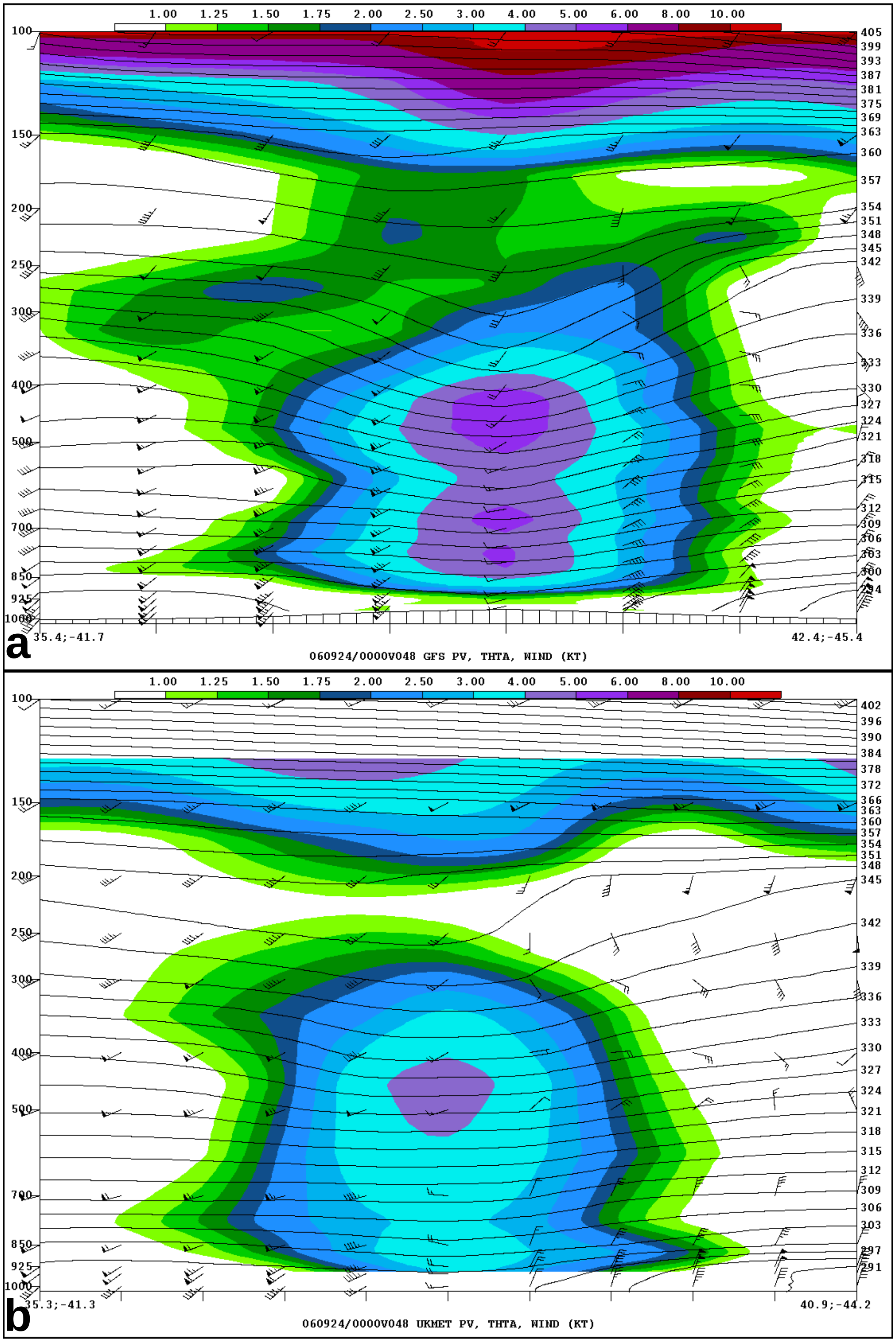


**Figure 15. As in Fig. 14., except 48-h forecast from (a) GFS along 35.4°N 41.7°W to 42.4°N 45.4°W and (b) UKMET along 35.3N 41.3W to 40.9N 44.2W valid at 0000 UTC 24 September.**